

Effect of Heat Transfer on Peristaltic Transport of a Johnson Segalman Fluid Through a Porous Medium in an Inclined Asymmetric Channel

Ali M. Kamal, Ahmed M. Abdulhadi

College of science, University of Baghdad, Baghdad- Iraq.

Abstract

In This paper the influence of heat transfer on peristaltic transport of Johnson Segalman fluid in an inclined asymmetric channel are investigated theoretically and graphically. A regular perturbation method is used to obtain the analytical solutions for the stream functions, temperature fields, axial pressure gradient, and pressure rise. The effects of the physical parameters of the problem on these distributions are discussed and illustrated graphically through a set of figures.

Keywords: Johnson Segalman fluid; Peristaltic transport; Heat transfer; Porous medium; Inclined asymmetric channel

1. Introduction

The Johnson- Segalman model is a viscoelastic fluid model which was developed to allow for non affine deformation [19]. Recently, this model has been used by a number of researchers [20,24,25] to explain the “spurt” phenomenon. Experimentalists usually associate a spurt with a slip at the wall, and on this issue experiments have been carried out [21,22,26,27,33]. Also Rao and Rajagopal [34] discussed three distinct flows of a Johnson-Segalman fluid. The three flows are cylindrical poiseuille flow. The mechanism of peristaltic transport has been exploited for industrial applications like sanitary fluid transport, blood pumps in heart lung machine and transport of corrosive fluids where the contact of the fluid with the machinery parts is prohibited. Since the first investigation of Latham [23], a number of analytical, numerical and experimental [1,2,3,6-10] studies of peristaltic flows of different fluid have been reported under different conditions with reference to physiological and mechanical situations. The peristaltic flows can be divided to Newtonian and non-Newtonian flows that have been reported analytically, numerically, and experimentally by a number of researchers [29-32]. Although most prior studies of peristaltic transport have focused on Newtonian fluids, there are also studies involving non-Newtonian fluid [11-15]. Srinivas and Pushparaj [36] discussed the non-linear peristaltic transport in an inclined asymmetric channel. Hayat et al. [26] investigated the peristaltic transport of a Johnson-Segalman fluid in an asymmetric channel. Reddy and Roju [35] studied the non-linear peristaltic pumping of Johnson-Segalman fluid in an asymmetric channel under the effect of a magnetic field. Recently, Hayat et. [16] discussed the peristaltic flow in an asymmetric channel for a J-S fluid and

previously the examiner Haroun [17] discussed the peristaltic flow in an inclined asymmetric channel for fourth grad fluid. He observed that with the increase in inclined angle the trapped bolus volume increase.

Considering the importance of heat transfer in peristaltic an attempt is made to study the combined effects of heat transfer and inclined angle on the peristaltic transport at a Johnson-Segalman fluid in an asymmetric channel. Nadeem and Noreen Sher Akbar [28] are studied the effect of heat transfer on peristaltic transport of a J-S fluid in an inclined asymmetric channel. El Shehawey and Husseny[4] and El Shehawey et al. [5] studied the peristaltic mechanism of a Newtonian fluid through a porous medium. Hall effects on peristaltic flow of a Maxwell fluid through a porous medium in a channel was studied by Hayat et. [18].

In the present note, a mathematical model is presented to understand the interaction between peristalsis and heat transfer for the motion of a viscous in compressible fluid in a tow-dimensional asymmetric inclined channel. The momentum and energy equations have been linearized under long –wavelength and low Reynold’s number assumptions and analytical solutions for the flow variables have been obtained.

2. The mathematical model

The constitutive equations for an incompressible Johnson-Segalman fluid are given by

2.1. Governing equations

Consider an incompressible, Johnson-Segalman fluid confined in a two-dimensional infinit inclined asymmetric channel of width d_1+d_2 (see Fig. 1). We consider an infinite wave train travelling with velocity c along the channel walls. The asymmetry in the channel is induced by assuming the peristaltic wave train on the walls to have different amplitudes and phase. The resulting asymmetric channel walls are defined as

$$Y = \bar{h}_1(\bar{X}, \bar{t}) = d_1 + a_1 \sin \left[\frac{2\pi}{\lambda} (\bar{X} - c\bar{t}) \right], \quad \text{upperwall}, \quad (1)$$

$$Y = \bar{h}_2(\bar{X}, \bar{t}) = -d_2 - a_2 \sin \left[\frac{2\pi}{\lambda} (\bar{X} - c\bar{t}) + \phi \right], \quad \text{lowerwall}. \quad (2)$$

Here a_1 and a_2 are the amplitude of the waves, λ is the wavelength and $\phi \in [0, \pi]$ is the phase difference. Note that $\phi = 0$ corresponds to an asymmetric channel with waves out of phase and $\phi = \pi$ describes the case where waves are in phase. Moreover a_1, a_2, d_1, d_2 and ϕ satisfy the following inqualit

$$a_1^2 + a_2^2 + 2a_1a_2 \cos \phi \leq (d_1 + d_2)^2 \quad (3)$$

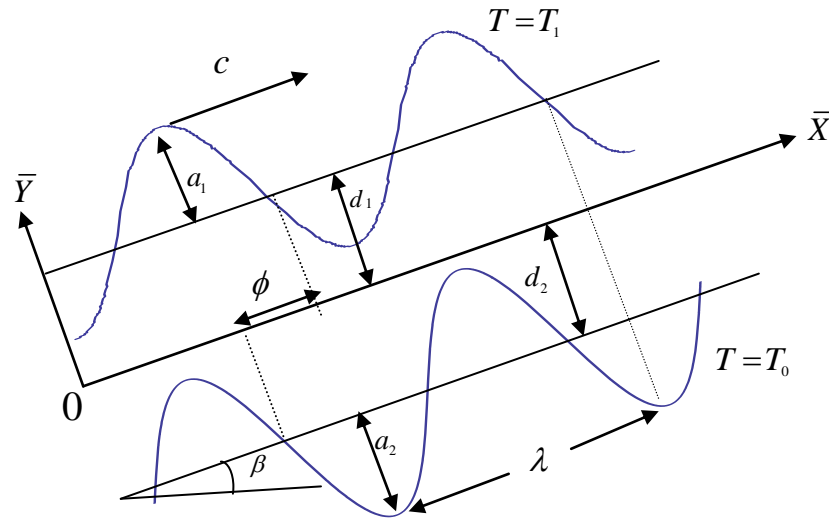


Fig.1. Schematic diagram of the problem

The equations governing the flow of an incompressible fluid are

$$\text{div } \bar{\mathbf{V}}=0, \quad \text{div } \bar{\boldsymbol{\sigma}} + \rho \bar{\mathbf{f}} = \rho \frac{d\bar{\mathbf{V}}}{dt}, \quad (4)$$

where $\bar{\mathbf{V}}$ is the velocity, $\bar{\mathbf{f}}$ is the body force per unit mass, ρ is the fluid density, $d/d\bar{t}$ is the material derivative and $\bar{\boldsymbol{\sigma}}$ is the cauchy stress tensor given by[19]

$$\bar{\boldsymbol{\sigma}} = -p\bar{\mathbf{I}} + \bar{\mathbf{T}}, \quad (5)$$

$$\bar{\mathbf{T}} = 2\mu\bar{\mathbf{D}} + \bar{\mathbf{S}}, \quad (6)$$

$$\bar{\mathbf{S}} + m \left[\frac{d\bar{\mathbf{S}}}{d\bar{t}} + \bar{\mathbf{S}}(\bar{\mathbf{W}} - e\bar{\mathbf{D}}) + (\bar{\mathbf{W}} - e\bar{\mathbf{D}})^T \bar{\mathbf{S}} \right] = 2\eta\bar{\mathbf{D}}, \quad (7)$$

$$\bar{\mathbf{D}} = \frac{1}{2}[\bar{\mathbf{L}} + \bar{\mathbf{L}}^T], \quad \bar{\mathbf{W}} = \frac{1}{2}[\bar{\mathbf{L}} - \bar{\mathbf{L}}^T], \quad \bar{\mathbf{L}} = \text{grad } \bar{\mathbf{V}} \quad (8)$$

and bars indicate the quantities in the dimensional coordinates. The equations above include the scalar pressure p , the identity tensor $\bar{\mathbf{I}}$, the extra stress $\bar{\mathbf{S}}$, the dynamic viscosities μ and η , the relaxation time m , the slip parameter e and the respective symmetric and skew symmetric part of the velocity gradient, $\bar{\mathbf{D}}$ and $\bar{\mathbf{W}}$. Note, that model (5) reduces to the Maxwell fluid model for $e=1$ and $\mu=0$, and for $m=0=\mu$ we receive the classical Navier-Stokes fluid model.

The velocity for unsteady tow-dimensional flows is defined as

$$\vec{V} = [\bar{U}(\bar{X}, \bar{Y}, \bar{t}), \bar{V}(\bar{X}, \bar{Y}, \bar{t}), 0]. \quad (9)$$

From Eqs. (4)-(9) we obtain,

$$\frac{\partial \bar{U}}{\partial \bar{X}} + \frac{\partial \bar{V}}{\partial \bar{Y}} = 0 \quad (10)$$

$$\rho \left(\frac{\partial}{\partial \bar{t}} + \bar{U} \frac{\partial}{\partial \bar{X}} + \bar{V} \frac{\partial}{\partial \bar{Y}} \right) \bar{U} = -\frac{\partial \bar{p}}{\partial \bar{X}} + \mu \left(\frac{\partial^2}{\partial \bar{X}^2} + \frac{\partial^2}{\partial \bar{Y}^2} \right) \bar{U} + \frac{\partial \bar{S}_{\bar{X}\bar{X}}}{\partial \bar{X}} + \frac{\partial \bar{S}_{\bar{X}\bar{Y}}}{\partial \bar{Y}} - \frac{\mu}{\kappa} \bar{U} + \rho g \sin \beta, \quad (11)$$

$$\rho \left(\frac{\partial}{\partial \bar{t}} + \bar{U} \frac{\partial}{\partial \bar{X}} + \bar{V} \frac{\partial}{\partial \bar{Y}} \right) \bar{V} = -\frac{\partial \bar{p}}{\partial \bar{Y}} + \mu \left(\frac{\partial^2}{\partial \bar{X}^2} + \frac{\partial^2}{\partial \bar{Y}^2} \right) \bar{V} + \frac{\partial^2 \bar{S}_{\bar{X}\bar{Y}}}{\partial \bar{X}^2} + \frac{\partial^2 \bar{S}_{\bar{Y}\bar{Y}}}{\partial \bar{Y}^2} - \frac{\mu}{\kappa} \bar{V} - \rho g \cos \beta, \quad (12)$$

$$2\eta \frac{\partial \bar{U}}{\partial \bar{X}} = \bar{S}_{\bar{X}\bar{X}} + m \left[\frac{\partial}{\partial \bar{t}} + \bar{U} \frac{\partial}{\partial \bar{X}} + \bar{V} \frac{\partial}{\partial \bar{Y}} \right] \bar{S}_{\bar{X}\bar{X}} - 2em\bar{S}_{\bar{X}\bar{X}} \frac{\partial \bar{U}}{\partial \bar{X}} + m \left[(1-e) \frac{\partial \bar{V}}{\partial \bar{X}} - (1+e) \frac{\partial \bar{U}}{\partial \bar{Y}} \right] \bar{S}_{\bar{X}\bar{Y}}, \quad (13)$$

$$\eta \left(\frac{\partial \bar{U}}{\partial \bar{Y}} + \frac{\partial \bar{V}}{\partial \bar{X}} \right) = \bar{S}_{\bar{X}\bar{Y}} + m \left[\frac{\partial}{\partial \bar{t}} + \bar{U} \frac{\partial}{\partial \bar{X}} + \bar{V} \frac{\partial}{\partial \bar{Y}} \right] \bar{S}_{\bar{X}\bar{Y}} + \frac{m}{2} \left[(1-e) \frac{\partial \bar{U}}{\partial \bar{Y}} - (1+e) \frac{\partial \bar{V}}{\partial \bar{X}} \right] \bar{S}_{\bar{X}\bar{X}} + \frac{m}{2} \left[(1-e) \frac{\partial \bar{V}}{\partial \bar{X}} - (1+e) \frac{\partial \bar{U}}{\partial \bar{Y}} \right] \bar{S}_{\bar{Y}\bar{Y}}, \quad (14)$$

$$2\eta \frac{\partial \bar{V}}{\partial \bar{Y}} = \bar{S}_{\bar{Y}\bar{Y}} + m \left[\frac{\partial}{\partial \bar{t}} + \bar{U} \frac{\partial}{\partial \bar{X}} + \bar{V} \frac{\partial}{\partial \bar{Y}} \right] \bar{S}_{\bar{Y}\bar{Y}} - 2em\bar{S}_{\bar{Y}\bar{Y}} \frac{\partial \bar{V}}{\partial \bar{Y}} + m \left[(1-e) \frac{\partial \bar{U}}{\partial \bar{Y}} - (1+e) \frac{\partial \bar{V}}{\partial \bar{X}} \right] \bar{S}_{\bar{X}\bar{Y}}, \quad (15)$$

$$\rho c_p \left(\frac{\partial T}{\partial \bar{t}} + \bar{U} \frac{\partial T}{\partial \bar{X}} + \bar{V} \frac{\partial T}{\partial \bar{Y}} \right) = \bar{S}_{\bar{X}\bar{X}} \frac{\partial \bar{U}}{\partial \bar{X}} + \bar{S}_{\bar{Y}\bar{Y}} \frac{\partial \bar{V}}{\partial \bar{Y}} + \bar{S}_{\bar{X}\bar{Y}} \left(\frac{\partial \bar{U}}{\partial \bar{Y}} + \frac{\partial \bar{V}}{\partial \bar{X}} \right) + k \left(\frac{\partial^2 T}{\partial \bar{X}^2} + \frac{\partial^2 T}{\partial \bar{Y}^2} \right). \quad (16)$$

In the fixed frame (\bar{X}, \bar{Y}) the motion is unsteady, while it becomes steady in the wave frame (\bar{x}, \bar{y}) given by

$$\bar{x} = \bar{X} - ct, \quad \bar{y} = \bar{Y}, \quad \bar{u} = \bar{U} - c, \quad \bar{v} = \bar{V}, \quad (17)$$

when moving away in direction of the wave from the fixed frame (\bar{X}, \bar{Y}) with speed c . Here \bar{u} , \bar{v} and \bar{U} , \bar{V} are the velocity components in the wave frame and in the fixed frame, respectively.

We put Eq. (17) into Eqs. (11)-(16) and to write continuity and motion equations in dimensionless form we introduce the following new quantities

$$\begin{aligned}
 x &= \frac{\bar{x}}{\lambda}, & y &= \frac{\bar{y}}{d_1}, & u &= \frac{\bar{u}}{c}, & v &= \frac{\bar{v}}{c}, & h_1 &= \frac{\bar{h}_1}{d_1}, & h_2 &= \frac{\bar{h}_2}{d_1}, \\
 S &= \frac{d_1}{\mu c} \bar{S}(\bar{x}), & p &= \frac{2\pi d_1^2}{\lambda(\mu+\eta)c} \bar{p}(\bar{x}), & \delta &= \frac{d_1}{\lambda}, & d &= \frac{d_2}{d_1}, \\
 a &= \frac{a_1}{d_1}, & b &= \frac{a_2}{d_1}, & R_e &= \frac{\rho c d_1}{\mu}, & W_i &= \frac{m c}{d_1}, & \bar{t} &= \frac{c t}{\lambda}, \\
 E_r &= \frac{e^2}{c_p(T_0 - T_1)}, & F_r &= \frac{c^2}{g d_1}, & P_r &= \frac{\rho c_p v}{k}, & \theta &= \frac{T - T_1}{T_0 - T_1}, & D_r &= \frac{k}{d_1^2},
 \end{aligned} \tag{18}$$

Where ρ is the density, μ is the coefficient of viscosity of the fluid, p is the pressure, β is the inclination of the channel with the horizontal, g is the acceleration due to gravity, T is the temperature, c_p is the specific heat at constant pressure and k is the thermal conductivity.

we have

$$\frac{\partial u}{\partial x} + \frac{\partial v}{\partial y} = 0, \tag{19}$$

$$\begin{aligned}
 R_e \delta \left(u \frac{\partial u}{\partial x} + v \frac{\partial u}{\partial y} \right) &= - \left(\frac{\mu + \eta}{\mu} \right) \frac{\partial p}{\partial x} + \delta^2 \frac{\partial^2 u}{\partial x^2} + \frac{\partial^2 u}{\partial y^2} + \delta \frac{\partial S_{xx}}{\partial x} + \frac{\partial S_{xy}}{\partial y} \\
 &\quad - \frac{1}{D_r} (u + 1) + \frac{R_e}{F_r} \sin \beta,
 \end{aligned} \tag{20}$$

$$\begin{aligned}
 R_e \delta^3 \left(u \frac{\partial v}{\partial x} + v \frac{\partial v}{\partial y} \right) &= - \left(\frac{\mu + \eta}{\mu} \right) \frac{\partial p}{\partial y} + \delta^2 \left[\delta^2 \frac{\partial^2 v}{\partial x^2} + \frac{\partial^2 v}{\partial y^2} \right] + \delta^2 \frac{\partial S_{xy}}{\partial y} \\
 &\quad + \delta \frac{\partial S_{yy}}{\partial y} - \frac{\delta^2}{D_r} v - \frac{R_e}{F_r} \cos \beta,
 \end{aligned} \tag{21}$$

$$\left(\frac{2\eta\delta}{\mu} \right) \frac{\partial u}{\partial x} = S_{xx} + W_i \delta \left[u \frac{\partial}{\partial x} + v \frac{\partial}{\partial y} \right] S_{xx} - 2e W_i \delta S_{xx} \frac{\partial u}{\partial x}$$

$$+W_i \left[\delta^2(1-e) \frac{\partial v}{\partial x} - (1+e) \frac{\partial u}{\partial y} \right] S_{xy}, \quad (22)$$

$$\begin{aligned} \frac{\eta}{\mu} \left(\frac{\partial u}{\partial y} + \delta^2 \frac{\partial v}{\partial x} \right) = S_{xy} + W_i \delta \left[u \frac{\partial}{\partial x} + v \frac{\partial}{\partial y} \right] S_{xy} + \frac{W_i}{2} \left[(1-e) \frac{\partial u}{\partial y} - (1+e) \delta^2 \frac{\partial v}{\partial x} \right] S_{xx} \\ + \frac{W_i}{2} \left[(1-e) \delta^2 \frac{\partial v}{\partial x} - (1+e) \frac{\partial v}{\partial x} \right] S_{yy}, \end{aligned} \quad (23)$$

$$\begin{aligned} \left(\frac{2\eta\delta}{\mu} \right) \frac{\partial v}{\partial y} = S_{yy} + W_i \delta \left[u \frac{\partial}{\partial x} + v \frac{\partial}{\partial y} \right] S_{yy} - 2eW_i \delta S_{yy} \frac{\partial v}{\partial y} \\ + \left[(1-e) \frac{\partial u}{\partial y} - (1+e) \delta^2 \frac{\partial v}{\partial x} \right] S_{xy} \end{aligned} \quad (24)$$

$$\begin{aligned} R_e \delta \left(u \frac{\partial \theta}{\partial x} + \delta v \frac{\partial \theta}{\partial y} \right) = E_r \left[S_{xx} \delta \frac{\partial u}{\partial x} + S_{xy} \delta \frac{\partial v}{\partial x} + S_{xy} \frac{\partial u}{\partial y} + S_{yy} \delta \frac{\partial v}{\partial y} \right] \\ + \frac{1}{P_r} \left[\delta^2 \frac{\partial^2 \theta}{\partial x^2} + \frac{\partial^2 \theta}{\partial y^2} \right]. \end{aligned} \quad (25)$$

Writing Eqs. (19)-(25) in terms of the stream function $\psi(x, y)$ defined by

$$u = \frac{\partial \psi}{\partial y}, \quad v = -\frac{\partial \psi}{\partial x}, \quad (26)$$

we get

$$\begin{aligned} \delta R_e \left[\left(\frac{\partial \psi}{\partial y} \frac{\partial}{\partial x} - \frac{\partial \psi}{\partial x} \frac{\partial}{\partial y} \right) \frac{\partial \psi}{\partial y} \right] = - \left(\frac{\mu + \eta}{\mu} \right) \frac{\partial p}{\partial x} + \delta^2 \frac{\partial^2 \psi}{\partial x \partial y} + \frac{\partial^3 \psi}{\partial y^3} + \delta \frac{\partial S_{xx}}{\partial x} \\ + \frac{\partial S_{xy}}{\partial y} - \frac{1}{D_r} \left(\frac{\partial \psi}{\partial y} + 1 \right) + \frac{R_e}{F_r} \sin \beta, \end{aligned} \quad (27)$$

$$\begin{aligned} -\delta^3 R_e \left[\left(\frac{\partial \psi}{\partial y} \frac{\partial}{\partial x} - \frac{\partial \psi}{\partial x} \frac{\partial}{\partial y} \right) \frac{\partial \psi}{\partial x} \right] = - \left(\frac{\mu + \eta}{\mu} \right) \frac{\partial p}{\partial y} - \delta^2 \left[\delta^2 \frac{\partial^3 \psi}{\partial x^3} + \frac{\partial^3 \psi}{\partial x \partial y^2} \right] + \delta^2 \frac{\partial S_{xy}}{\partial x} \\ + \delta \frac{\partial S_{yy}}{\partial y} \frac{\delta^2}{D_r} + \frac{\partial \psi}{\partial x} - \delta \frac{R_e}{F_r} \cos \beta, \end{aligned} \quad (28)$$

$$\left(\frac{2\eta\delta}{\mu}\right)\frac{\partial^2\psi}{\partial x\partial y} = S_{xx} + W_i\delta\left[\left(\frac{\partial\psi}{\partial y}\frac{\partial}{\partial x} - \frac{\partial\psi}{\partial x}\frac{\partial}{\partial y}\right)\right]S_{xx} - 2eW_i\delta\frac{\partial^2\psi}{\partial x\partial y} - W_i\left[\delta^2(1-e)\frac{\partial^2\psi}{\partial x^2} + (1+e)\frac{\partial^2\psi}{\partial y^2}\right]S_{xy}, \quad (29)$$

$$\frac{\eta}{\mu}\left(\frac{\partial^2\psi}{\partial y^2} - \delta^2\frac{\partial^2\psi}{\partial x^2}\right) - S_{xy} + W_i\delta\left[\left(\frac{\partial\psi}{\partial y}\frac{\partial}{\partial x} - \frac{\partial\psi}{\partial x}\frac{\partial}{\partial y}\right)\right]S_{xy} + \frac{W_i}{2}\left[(1-e)\frac{\partial^2\psi}{\partial y^2} + \delta^2(1+e)\frac{\partial^2\psi}{\partial x^2}\right]S_{xx} + \frac{W_i}{2}\left[\delta^2(1-e)\frac{\partial^2\psi}{\partial x^2} + (1+e)\frac{\partial^2\psi}{\partial y^2}\right]S_{yy}, \quad (30)$$

$$\left(\frac{2\eta\delta}{\mu}\right)\frac{\partial^2\psi}{\partial x\partial y} = S_{yy} + W_i\delta\left[\left(\frac{\partial\psi}{\partial y}\frac{\partial}{\partial x} - \frac{\partial\psi}{\partial x}\frac{\partial}{\partial y}\right)\right]S_{yy} + 2eW_i\delta S_{yy}\frac{\partial^2\psi}{\partial x\partial y} + W_i\left[(1-e)\frac{\partial^2\psi}{\partial y^2} + \delta^2(1+e)\frac{\partial^2\psi}{\partial x^2}\right]S_{xy}, \quad (31)$$

$$\delta R_e\left[\left(\frac{\partial\psi}{\partial y}\frac{\partial\theta}{\partial x} - \delta\frac{\partial\psi}{\partial x}\frac{\partial\theta}{\partial y}\right)\right] = E_r\left[S_{xx}\delta\frac{\partial^2\psi}{\partial x\partial y} - S_{xy}\delta\frac{\partial^2\psi}{\partial x^2} + S_{xy}\frac{\partial^2\psi}{\partial y^2} - S_{yy}\delta\frac{\partial^2\psi}{\partial x\partial y}\right] + \frac{1}{P_r}\left(\delta^2\frac{\partial^2\theta}{\partial x^2} + \frac{\partial^2\theta}{\partial y^2}\right). \quad (32)$$

where δ is wave number, R_e is the Renold's number, W_i is the Weissenberg number, F_r is the Froud number, P_r is the Prandtl number and D_r is the Darcy number. The continuity equation is identically satisfied.

2.2 Rate of volume flow and boundary conditions

The dimensional rate of fluid flow in the fixed frame (\bar{X}, \bar{Y}) is

$$Q = \int_{\bar{h}_1(\bar{x})}^{\bar{h}_2(\bar{x})} \bar{U}(\bar{X}, \bar{Y}, \bar{t}) d\bar{Y} \quad (33)$$

In the wave frame (\bar{x}, \bar{y}) Eq. (33) reduces to

$$q = \int_{\bar{h}_1(\bar{x})}^{\bar{h}_2(\bar{x})} \bar{u}(\bar{x}, \bar{y}) d\bar{y} \quad (34)$$

By Eq.(17), the above rates are related in the following expression

$$Q = q + c\bar{h}_1 - c\bar{h}_2 \quad (35)$$

Applying the averaged flow

$$\bar{Q} = \frac{1}{\tau} \int_0^{\tau} Q dt \quad (36)$$

Over a period ($\tau = \lambda \setminus c$) at a fixed position \bar{X} , we receive

$$Q = q + c\bar{d}_1 - c\bar{d}_2. \quad (37)$$

With the definition of the dimensionless time averaged flows

$$\Theta \equiv \frac{\bar{Q}}{cd_1}, \quad F \equiv \frac{q}{cd_1}, \quad (38)$$

in the fixed and moving frames, respectively, we can write Eq(37) as

$$\Theta = F + 1 + d \quad (39)$$

where

$$F = \int_{h_1(x)}^{h_2(x)} \frac{\partial \psi}{\partial y} dy = \psi(h_1) - \psi(h_2) \quad (40)$$

and the dimensionless surface of the peristaltic walls are

$$h_1(x) = 1 + a \sin(2\pi x), \quad h_2(x) = -d - b \sin(2\pi x + \phi), \quad (41)$$

where the inequality

$$a^2 + b^2 + 2ab \cos \phi \leq (1 + d)^2 \quad (42)$$

holds. The dimensionless boundary conditions in the wave frame are

$$\left. \begin{aligned} \psi &= \frac{F}{2}, & \frac{\partial \psi}{\partial y} &= -1 & \text{at } y &= h_1(x), \\ \psi &= -\frac{F}{2}, & \frac{\partial \psi}{\partial y} &= -1 & \text{at } y &= h_2(x) \\ \theta &= 1 & \text{at } y &= h_1(x), & \theta &= 0 & \text{at } y &= h_2(x), \end{aligned} \right\} \quad (43)$$

Here it is pointed out that the conditions on ψ satisfy Eq. (40) and the conditions on $\frac{\partial \psi}{\partial y}$ are no-slip .

2.3 Model equations

under lubrication approach(i.e., neglecting the terms of order δ and Re), from Eqs. (27)-(32) we get

$$\left(\frac{\mu + \eta}{\eta} \right) \frac{\partial p}{\partial x} = \frac{\partial S_{xy}}{\partial y} + \frac{\partial^3 \psi}{\partial y^3} - \frac{1}{D_r} \left(\frac{\partial \psi}{\partial y} + 1 \right) + \frac{R_e}{F_r} \sin \beta, \quad (44)$$

$$\frac{\partial p}{\partial y} = 0, \quad (45)$$

$$S_{xx} = W_i (1 + e) \frac{\partial^2 \psi}{\partial y^2} S_{xy}, \quad (46)$$

$$\left(\frac{\eta}{\mu} \right) \left(\frac{\partial^2 \psi}{\partial y^2} \right) = S_{xy} + \frac{W_i}{2} (1 - e) \frac{\partial^2 \psi}{\partial y^2} S_{xx} - \frac{W_i}{2} (1 + e) \frac{\partial^2 \psi}{\partial y^2} S_{yy}, \quad (47)$$

$$S_{yy} = -W_i (1 - e) \frac{\partial^2 \psi}{\partial y^2} S_{xy}, \quad (48)$$

$$E_r P_r S_{xy} \frac{\partial^2 \psi}{\partial y^2} + \frac{\partial^2 \theta}{\partial y^2} = 0, \quad (49)$$

From Eqs. (46)-(48), we write

$$S_{xy} = \frac{\left(\frac{\eta}{\mu} \right) \left(\frac{\partial^2 \psi}{\partial y^2} \right)}{1 + W_i^2 (1 - e^2) \left(\frac{\partial^2 \psi}{\partial y^2} \right)^2}, \quad (50)$$

using Eqs.(46),(48) and (50), the Eq.(44) and (49) can be rewritten as

$$\frac{\partial^2}{\partial y^2} \left[\frac{\left(\frac{\eta}{\mu} + 1 \right) \frac{\partial^2 \psi}{\partial y^2} + W_i^2 (1 - e^2) \left(\frac{\partial^2 \psi}{\partial y^2} \right)^3}{1 + W_i^2 (1 - e^2) \left(\frac{\partial^2 \psi}{\partial y^2} \right)^2} \right] = 0, \quad (51)$$

$$\frac{\partial p}{\partial x} = \frac{\partial^3 \psi}{\partial y^3} + W_i^2 \alpha_1 \frac{\partial}{\partial y} \left[\left(\frac{\partial^2 \psi}{\partial y^2} \right)^3 \right] - \frac{\mu}{(\mu + \eta) D_r} \frac{\partial \psi}{\partial y} + \left(\frac{\mu}{\mu + \eta} \right) \frac{R_e}{F_r} \sin \beta, \quad (52)$$

$$\frac{\partial^2 \theta}{\partial y^2} = -E_r P_r \left[\frac{\eta}{\mu} \left(\frac{\partial^2 \psi}{\partial y^2} \right)^2 - W_i^2 \frac{\eta}{\mu} (1 - e^2) \left(\frac{\partial^2 \psi}{\partial y^2} \right)^4 \right], \quad (53)$$

where $\alpha_1 = \frac{(e^2 - 1)\eta}{(\eta + \mu)}$

3. perturbed systems and perturbation solutions

The Eqs. (51)-(53) are non-linear and its closed form solution is not possible. thus, we linearize this equations in terms of W_i^2 since W_i is small for the type of flow under consideration. So we expand ψ, p, F and θ as

$$\begin{aligned} \psi &= \psi_0 + W_i^2 \psi_1 + O(W_i^4), \\ p &= p_0 + W_i^2 p_1 + O(W_i^4), \\ F &= F_0 + W_i^2 F_1 + O(W_i^4), \\ \theta &= \theta_0 + W_i^2 \theta_1 + O(W_i^4), \end{aligned} \quad (54)$$

substituting Eq.(54) into Eqs. (51)-(53) and boundary conditions (43), then equating the like powers of W_i^2 we get :

3.1. perturbed systems

3.1.1. Zeroth-order system

$$\left. \begin{aligned} \frac{\partial^4 \psi_0}{\partial y^4} &= \frac{\mu}{(\mu + \eta) D_r} \frac{\partial^2 \psi_0}{\partial y^2}, \\ \frac{\partial p_0}{\partial y} &= 0, \\ \frac{\partial p_0}{\partial x} &= \frac{\partial^3 \psi_0}{\partial y^3} - \frac{\mu}{(\mu + \eta) D_r} \frac{\partial \psi_0}{\partial y} + \left(\frac{\mu}{\mu + \eta} \right) \frac{R_e}{F_r} \sin \beta, \\ \frac{\partial^2 \theta_0}{\partial y^2} &= -E_r P_r \left[\frac{\eta}{\mu} \left(\frac{\partial^2 \psi_0}{\partial y^2} \right)^2 \right], \end{aligned} \right\} \quad (55)$$

$$\left. \begin{aligned} \psi_0 &= \frac{F_0}{2}, & \frac{\partial \psi_0}{\partial y} &= -1, & \text{at } y &= h_1(x), \\ \psi_0 &= -\frac{F_0}{2}, & \frac{\partial \psi_0}{\partial y} &= -1, & \text{at } y &= h_2(x), \\ \theta_0 &= 1, & \text{at } y &= h_1(x), & \theta_0 &= 0, & \text{at } y &= h_2(x), \end{aligned} \right\} \quad (56)$$

3.1.2. First –order system

$$\left. \begin{aligned} \frac{\partial^4 \psi_1}{\partial y^4} &= \frac{\mu}{(\mu + \eta) D_r} \frac{\partial^2 \psi_1}{\partial y^2} - \alpha_1 \frac{\partial^2}{\partial y^2} \left[\left(\frac{\partial^2 \psi_0}{\partial y^2} \right)^3 \right], \\ \frac{\partial p_1}{\partial y} &= 0, \\ \frac{\partial p_1}{\partial x} &= \frac{\partial^3 \psi_1}{\partial y^3} + \alpha_1 \frac{\partial}{\partial y} \left[\left(\frac{\partial^2 \psi_0}{\partial y^2} \right)^3 \right] - \frac{\mu}{(\mu + \eta) D_r} \frac{\partial \psi_1}{\partial y}, \\ \frac{\partial^2 \theta_1}{\partial y^2} &= -E_r P_r \left[\frac{2\eta}{\mu} \frac{\partial^2 \psi_0}{\partial y^2} \frac{\partial^2 \psi_1}{\partial y^2} - \frac{\eta}{\mu} (1 - e^2) \left(\frac{\partial^2 \psi_0}{\partial y^2} \right)^4 \right], \end{aligned} \right\} \quad (57)$$

$$\left. \begin{aligned} \psi_1 &= \frac{F_1}{2}, & \frac{\partial \psi_1}{\partial y} &= 0, & \text{at } y &= h_1(x), \\ \psi_1 &= -\frac{F_1}{2}, & \frac{\partial \psi_1}{\partial y} &= 0, & \text{at } y &= h_2(x), \\ \theta_1 &= 0, & \text{at } y &= h_1(x), & \theta_1 &= 0 & \text{at } y &= h_2(x), \end{aligned} \right\} \quad (58)$$

3.2 Perturbation solutions

3.2.1. Zeroth-order solution

The solution of Eqs.(55) of zeroth order system, satisfying (56) can be written

$$\psi_0 = A_7 + A_8 y + \frac{(A_5 + A_6) \cosh(\sqrt{A_1} y) + (A_5 - A_6) \sinh(\sqrt{A_1} y)}{A_1}, \quad (59)$$

$$\frac{dp_0}{dx} = A_2 - A_1 A_8, \quad (60)$$

$$\theta_0 = \frac{A_3(\cosh(2\sqrt{A_1} y) - \sinh(2\sqrt{A_1} y))(A_6^2 + A_5^2(\cosh(4\sqrt{A_1} y) + \sinh(4\sqrt{A_1} y)))}{4A_1} + \frac{4A_1(A_9 + y(A_{10} + A_3A_5A_6y))}{4A_1}. \quad (61)$$

where

$$A_1 = \frac{\mu}{(\mu + \eta)D_r}, \quad A_2 = \frac{\mu R_e \sin(\beta)}{(\mu + \eta)F_r}, \quad A_3 = \frac{-E_r P_r \eta}{\mu},$$

A_5, A_6, A_7, A_8, A_9 and A_{10} are constants can be determinates by using the boundary conditions Eq.(56) .

3.2.2. First-order solution

Substituting the zeroth-order solution (59)-(61) into Eq.(57) and then solving the resulting system with the corresponding boundary conditions Eq.(58),we get

$$\begin{aligned} \psi_1 = & B_3 + B_4 y + \frac{1}{8A_1} (8((B_1 + B_2) \cosh(\sqrt{A_1} y) + (B_1 - B_2) \sinh(\sqrt{A_1} y)) \\ & - 6A_5 A_6 (A_5(-5 + 2\sqrt{A_1} y) - A_6(5 + 2\sqrt{A_1} y)) \cosh(\sqrt{A_1} y) \\ & + (A_5^3 + A_6^3) \cosh(3\sqrt{A_1} y) + (A_5^3 - A_6^3 + 6A_5^2 A_6(-5 + 2\sqrt{A_1} y) \\ & + 6A_5 A_6^2(5 + 2\sqrt{A_1} y) + 2(A_5^3 - A_6^3) \cosh(2\sqrt{A_1} y)) \sinh(\sqrt{A_1} y)) \alpha_1, \end{aligned} \quad (62)$$

$$\frac{dp_1}{dx} = -A_1 B_4, \quad (63)$$

$$\begin{aligned} \theta_1 = & B_5 + \frac{1}{4} \left((4B_6 y + 4A_3 B_1 B_2 y^2 - 4A_4 \cosh(\sqrt{A_1} y) - \sinh(\sqrt{A_1} y)) \right. \\ & \left. (A_6 + A_5 \cosh(2\sqrt{A_1} y) + A_5 \sinh(2\sqrt{A_1} y)) \right. \\ & \left. + \frac{1}{4A_1} A_3 (\cosh(2\sqrt{A_1} y) - \sinh(2\sqrt{A_1} y)) \right. \\ & \left. (B_2^2 + B_1^2 \cosh(4\sqrt{A_1} y) + B_1^2 \sinh(4\sqrt{A_1} y)) \right) \end{aligned}$$

$$\begin{aligned}
 & + \frac{1}{256A_1} A_3 (\cosh(6\sqrt{A_1} y) - \sinh(6\sqrt{A_1} y)) \alpha_1 \\
 & (9A_6^6 \alpha_1 + 9A_5^6 \cosh(12\sqrt{A_1} y) \alpha_1 + 9A_5^6 \sinh(12\sqrt{A_1} y) \alpha_1 \\
 & + 18A_5^3 (\cosh(10\sqrt{A_1} y) + \sinh(10\sqrt{A_1} y)) (-2B_1 - 3A_5^2 A_6 \alpha_1 + 3\sqrt{A_1} A_5^2 A_6 y \alpha_1) \\
 & - 18A_6^3 (\cosh(2\sqrt{A_1} y) + \sinh(2\sqrt{A_1} y)) (2B_2 + 3A_5 A_6^2 \alpha_1 + 3\sqrt{A_1} A_5 A_6^2 y \alpha_1) \\
 & + 24A_5^2 (\cosh(8\sqrt{A_1} y) + \sinh(8\sqrt{A_1} y)) (-6B_2 A_5 + 12B_1 A_6 - 8\sqrt{A_1} B_1 A_6 y + 21A_5^2 A_6^2 \alpha_1 \\
 & - 27\sqrt{A_1} A_5^2 A_6^2 \alpha_1 + 6A_1 A_5^2 A_6^2 y^2 \alpha_1) + 24A_6^2 (\cosh(4\sqrt{A_1} y) \\
 & + \sinh(4\sqrt{A_1} y)) (12B_2 A_5 - 6B_1 A_6 + 8\sqrt{A_1} B_2 A_5 y \\
 & + 21A_5^2 A_6^2 \alpha_1 + 27\sqrt{A_1} A_5^2 A_6^2 \alpha_1 + 6A_1 A_5^2 A_6^2 y^2 \alpha_1) \\
 & - 4A_1 A_5 A_6 y^2 (\cosh(6\sqrt{A_1} y) + \sinh(6\sqrt{A_1} y)) \\
 & (-48B_2 A_5 - 48B_1 A_6 + 32\sqrt{A_1} B_2 A_5 y - 32\sqrt{A_1} B_1 A_6 y \\
 & - 117A_5^2 A_6^2 \alpha_1 + 24A_1 A_5^2 A_6^2 y^2 \alpha_1) \tag{64}
 \end{aligned}$$

Where

$$\alpha_1 = \frac{(n^2 - 1)\eta}{(\mu + \eta)}, \quad A_4 = A_3(1 - n^2),$$

B_1, B_2, B_3, B_4, B_5 and B_6 are constants can be determinates by using the boundary conditions Eq. (58) .

Summing up the perturbation results, we find that

$$\begin{aligned}
 \psi & = A_7 + A_8 y + \frac{(A_5 + A_6) \cosh(\sqrt{A_1} y) + (A_5 - A_6) \sinh(\sqrt{A_1} y)}{A_1} \\
 W_i & (B_3 + B_4 y + \frac{1}{8A_1} (8((B_1 + B_2) \cosh(\sqrt{A_1} y) + (B_1 - B_2) \sinh(\sqrt{A_1} y)))
 \end{aligned}$$

$$\begin{aligned}
 & -6A_5A_6(A_5(-5+2\sqrt{A_1}y) - A_6(5+2\sqrt{A_1}y)) \cosh(\sqrt{A_1}y) \\
 & + (A_5^3 + A_6^3) \cosh(3\sqrt{A_1}y) + (A_5^3 - A_6^3 + 6A_5^2A_6(-5+2\sqrt{A_1}y) \\
 & + 6A_5A_6^2(5+2\sqrt{A_1}y) + 2(A_5^3 - A_6^3) \cosh(2\sqrt{A_1}y)) \sinh(\sqrt{A_1}y) \alpha_1, \tag{65}
 \end{aligned}$$

$$\frac{dp}{dx} = A_2 - A_1A_8 - Wi(A_1B_4), \tag{66}$$

$$\begin{aligned}
 \theta = & \frac{A_3(\cosh(2\sqrt{A_1}y) - \sinh(2\sqrt{A_1}y))(A_6^2 + A_5^2(\cosh(4\sqrt{A_1}y) + \sinh(4\sqrt{A_1}y)))}{4A_1} \\
 & + Wi \left(B_5 + \frac{1}{4} \left((4B_6y + 4A_3B_1B_2y^2 - 4A_4 \cosh(\sqrt{A_1}y) - \sinh(\sqrt{A_1}y)) \right. \right. \\
 & \left. \left. (A_6 + A_5 \cosh(2\sqrt{A_1}y) + A_5 \sinh(2\sqrt{A_1}y)) \right. \right. \\
 & \left. \left. + \frac{1}{4A_1} A_3 (\cosh(2\sqrt{A_1}y) - \sinh(2\sqrt{A_1}y)) \right. \right. \\
 & \left. \left. (B_2^2 + B_1^2 \cosh(4\sqrt{A_1}y) + B_1^2 \sinh(4\sqrt{A_1}y)) \right) \right) \\
 & + \frac{1}{256A_1} A_3 (\cosh(6\sqrt{A_1}y) - \sinh(6\sqrt{A_1}y)) \alpha_1 \\
 & (9A_6^6 \alpha_1 + 9A_5^6 \cosh(12\sqrt{A_1}y) \alpha_1 + 9A_5^6 \sinh(12\sqrt{A_1}y) \alpha_1 \\
 & + 18A_5^3 (\cosh(10\sqrt{A_1}y) + \sinh(10\sqrt{A_1}y)) (-2B_1 - 3A_5^2 A_6 \alpha_1 + 3\sqrt{A_1} A_5^2 A_6 y \alpha_1) \\
 & - 18A_6^3 (\cosh(2\sqrt{A_1}y) + \sinh(2\sqrt{A_1}y)) (2B_2 + 3A_5 A_6^2 \alpha_1 + 3\sqrt{A_1} A_5 A_6^2 y \alpha_1) \\
 & + 24A_5^2 (\cosh(8\sqrt{A_1}y) + \sinh(8\sqrt{A_1}y)) (-6B_2 A_5 + 12B_1 A_6 - 8\sqrt{A_1} B_1 A_6 y + 21A_5^2 A_6^2 \alpha_1 \\
 & - 27\sqrt{A_1} A_5^2 A_6^2 \alpha_1 + 6A_1 A_5^2 A_6^2 y^2 \alpha_1) + 24A_6^2 (\cosh(4\sqrt{A_1}y) \\
 & + \sinh(4\sqrt{A_1}y)) (12B_2 A_5 - 6B_1 A_6 + 8\sqrt{A_1} B_2 A_5 y \\
 & + 21A_5^2 A_6^2 \alpha_1 + 27\sqrt{A_1} A_5^2 A_6^2 \alpha_1 + 6A_1 A_5^2 A_6^2 y^2 \alpha_1)
 \end{aligned}$$

$$\begin{aligned}
 & -4A_1A_3A_6y^2(\cosh(6\sqrt{A_1}y) + \sinh(6\sqrt{A_1}y)) \\
 & (-48B_2A_5 - 48B_1A_6 + 32\sqrt{A_1}B_2A_5y - 32\sqrt{A_1}B_1A_6y \\
 & -117A_5^2A_6^2\alpha_1 + 24A_1A_5^2A_6^2y^2\alpha_1)) \quad (67)
 \end{aligned}$$

The non dimensional pressure rise per wavelength ΔP is defined as

$$\Delta P = \int_0^1 \frac{dp}{dx} dx, \quad (68)$$

Where $\frac{dp}{dx}$ is defined through Eq.(66).

Not that, if we assume that the Darcy number was closer to infinity, then the results of the problem reduce exactly to the same as that found by Nadeem and Akbar [28].

4. Results and discussions

This section represents the graphical results in order to be able to discuss the quantitative effects of the sundry parameters involved in the analysis .

4.1. Pumping characteristics

We plot the expression for ΔP in Eq. (68) against Θ for various values of parameters of interest in Figs.(2-9). In Fig.2 the effects of region channel width d on ΔP are seen. Observe that , in the pumping ($\Delta P > 0$) and free pumping ($\Delta P = 0$) for the J-S fluid, an increase in d causes a decrease in pumping. While in the co-pumping ($\Delta P < 0$), the pumping increases with an increase in d . Fig.3 the effects of Weissenberg number on ΔP . Observe that an increase in W_i causes a decrease in the pumping region ($\Delta P > 0$) and behaves oppositely in the free pumping ($\Delta P = 0$) and co-pumping. The observations regarding the effects of upper and lower wave amplitudes b and a (Fig.4 and 5) on ΔP are quite opposite to those in the case of phase difference ϕ Fig.7. Observe that an increase in ϕ causes a decrease in the pumping region ($\Delta P > 0$). It is also noted from Fig.7 that in free pumping and co-pumping ΔP increases with an increase in ϕ . The effects of F_r on pressure rise ΔP are illustrated in Fig.6. It is seen that with the increase in F_r the pressure rise decreases in the all pumping regions ($\Delta P > 0$), ($\Delta P = 0$) and ($\Delta P < 0$). The pressure rise increases with increase in β and D_r . But this increasing in ΔP occurs in the co-pumping region which are displayed in (Fig.8 and 9) respectively.

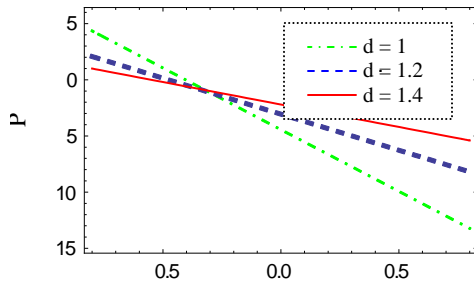


Fig.2. Effect of the width of channel d on variation of Δp versus Θ for : $a=0.5$, $b=0.4$, $W_i=0.25$, $\phi=0.2$, $\mu=0.03$, $\eta=0.04$, $d=0.5$, $D_r=1$, $F_r=1$, $R_e=10$, $\beta=0.5$, $e=0.2$.

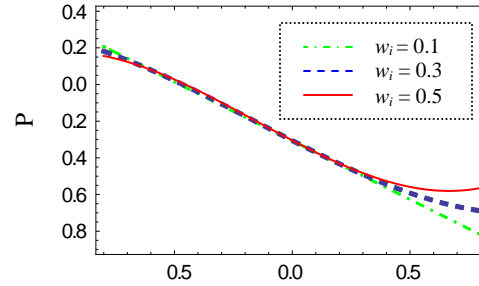


Fig.3. Effect of the Weisenberg number W_i on variation of Δp versus Θ for : $a=0.5$, $\phi=0.2$, $\mu=0.03$, $\eta=0.04$, $d=0.9$, $D_r=1$, $F_r=1$, $R_e=10$, $\beta=0.5$, $e=0.2$.

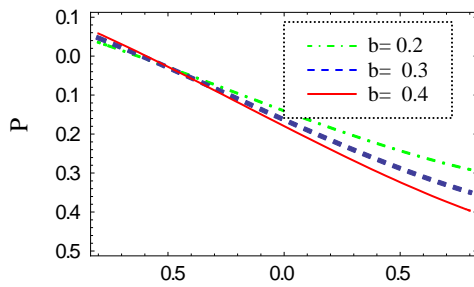


Fig.4. Effect of the lower wave amplitude b on variation of Δp versus Θ for : $a=0.5$, $\phi=0.2$, $\mu=0.03$, $\eta=0.04$, $W_i=0.25$, $d=0.5$, $D_r=1$, $F_r=1$, $R_e=10$, $\beta=0.5$, $e=0.2$.

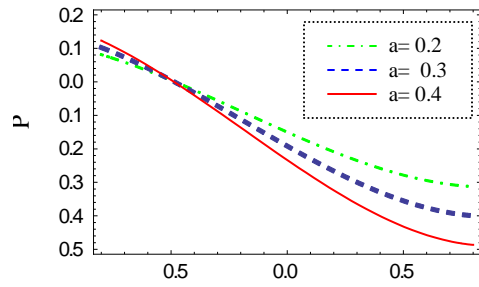


Fig.5. Effect of the upper wave amplitude a on variation of Δp versus Θ for : $b=0.5$, $\phi=0.5$, $\mu=0.03$, $\eta=0.04$, $W_i=0.01$, $d=0.1$, $D_r=1$, $F_r=1$, $R_e=10$, $\beta=0.5$, $e=0.2$.

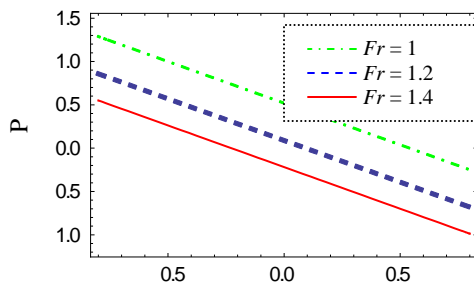


Fig.6. Effect of the Froud number F_r on variation of Δp versus Θ for : $b=0.5$, $a=0.5$, $\mu=0.03$, $\eta=0.04$, $W_i=0.01$, $d=0.1$, $D_r=1$, $\phi=0.2$, $R_e=10$, $\beta=0.5$, $e=0.2$.

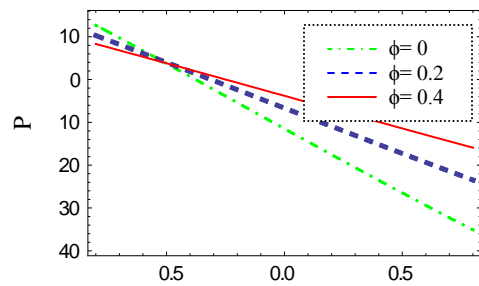


Fig.7. Effect of the phase difference ϕ on variation of Δp versus Θ for : $b=0.5$, $a=0.5$, $\mu=0.03$, $\eta=0.04$, $W_i=0.01$, $d=0.1$, $D_r=1$, $F_r=1$, $R_e=10$, $e=0.2$.

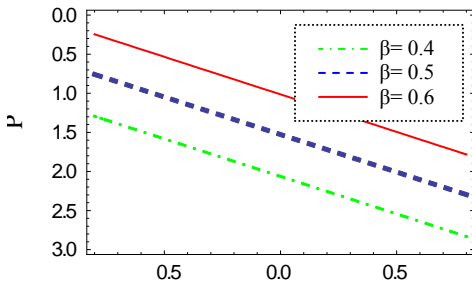


Fig.8. Effect of inclined angle β on variation of Δp versus Θ for :
 $b=0.5, a=0.5, \mu=0.03, \eta=0.04, W_i=0.01,$
 $d=3.5, D_r=1, F_r=1, R_e=10, \phi=0.2, e=0.2.$

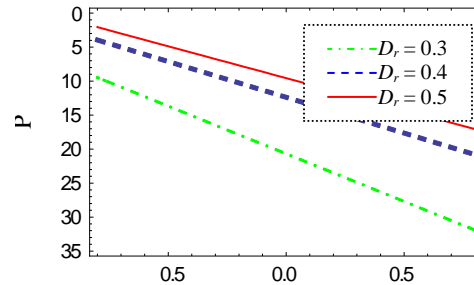


Fig.9. Effect of the Darcy number F_r on variation of Δp versus Θ for :
 $b=0.5, a=0.5, \mu=0.03, \eta=0.04, W_i=0.01,$
 $d=0.1, F_r=1, \phi=0.2, R_e=10, \beta=0.5, e=0.2.$

4.2. Pressure gradient characteristics

The variation of the axial pressure gradient dp/dx with x for various values $\phi, a, b, \mu, \eta, d, D_r, F_r, R_e, \beta, \Theta$ and W_i are shown in Figs.(10-21). Fig.10 studies the effects of phase shift ϕ on the variation of pressure gradient dp/dx , and it is noticed that the axial pressure gradient decreases by increasing ϕ . Fig.11 and 12 shows the variation of the axial pressure gradient dp/dx with b and a respectively. It is clear that the axial pressure gradient increases with an increase in amplitudes of the waves. Fig.13 shows the effect of μ on dp/dx . It is noted that, the magnitude of dp/dx increase with increasing μ and verse to versa in Fig.14 the magnitude of dp/dx decreases with increasing η . The effect the Weissenberg number W_i on the variation of pressure gradient dp/dx with x is shown in Fig.15. It is observed that, the magnitude of the dp/dx increases with increasing W_i . Fig.(16-21) illustrates the variation of the axial pressure gradient dp/dx with x for different values of D_r, β, d, R_e, F_r and Θ . It is clear that the axial pressure gradient dp/dx decreases with an increase in D_r Fig.16. Also dp/dx increases by increasing β and R_e (Fig.17 and 19). The situation is reversed in Figs.18, 20 and 21, the axial pressure gradient is decreased with an increase in d, F_r and Θ .

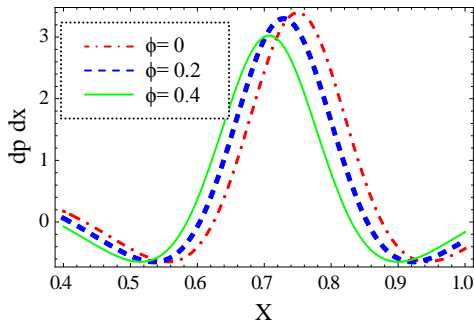


Fig.10. Effect of ϕ on the variation of pressure gradient dp/dx with x : $b=0.4, a=0.2, \mu=1, \eta=1, W_i=0.01, D_r=0.5, F_r=1, R_e=10, \beta=0.5, d=0.3, e=0.8, \Theta=0.6$.

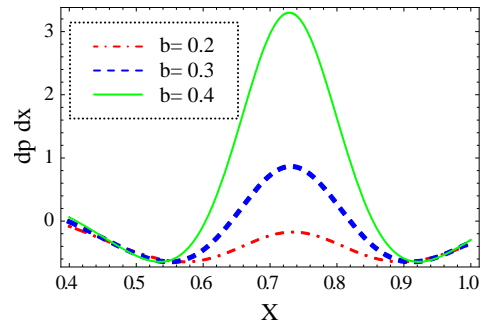


Fig.11. Effect of b on the variation of pressure gradient dp/dx with x : $\phi=0.2, a=0.2, \mu=1, \eta=1, W_i=0.01, D_r=0.5, F_r=1, R_e=10, \beta=0.5, d=0.3, e=0.8, \Theta=0.6$.

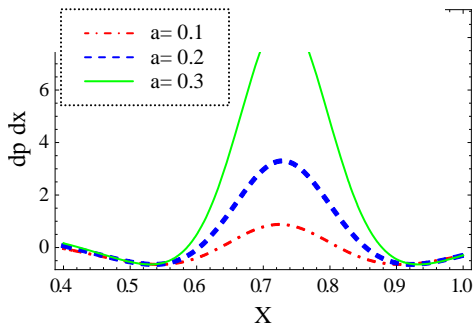


Fig.12. Effect of a on the variation of pressure gradient dp/dx with x : $b=0.4, \phi=0.2, \mu=1, \eta=1, W_i=0.01, D_r=0.5, F_r=1, R_e=10, \beta=0.5, d=0.3, e=0.8, \Theta=0.6$.

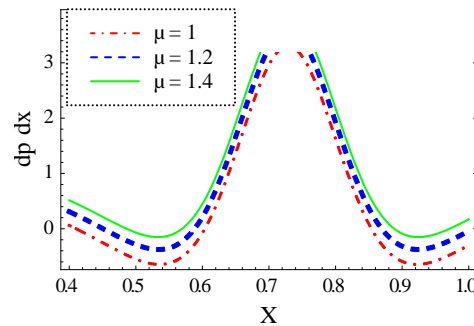


Fig.13. Effect of μ on the variation of pressure gradient dp/dx with x : $b=0.4, a=0.2, \phi=0.2, \eta=1, W_i=0.01, D_r=0.5, F_r=1, R_e=10, \beta=0.5, d=0.3, e=0.8, \Theta=0.6$.

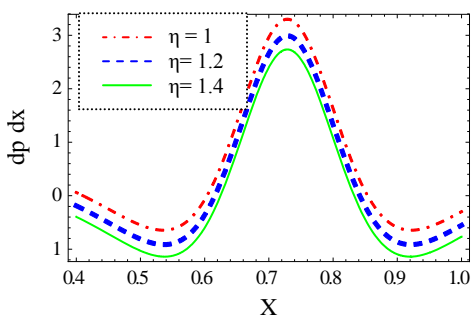


Fig.14. Effect of η on the variation of pressure gradient dp/dx with x : $b=0.4, a=0.2, \mu=1, \phi=0.2, W_i=0.01, D_r=0.5, F_r=1, R_e=10, \beta=0.5, d=0.3, e=0.8, \Theta=0.6$.

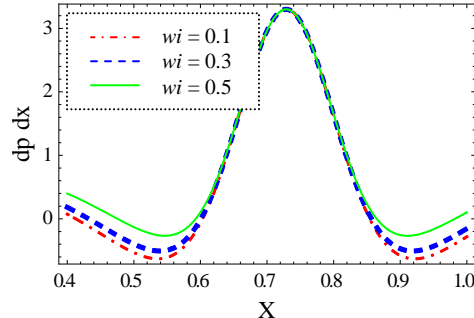


Fig.15. Effect of W_i on the variation of pressure gradient dp/dx with x : $b=0.4, a=0.2, \mu=1, \eta=1, \phi=0.2, D_r=0.5, F_r=1, R_e=10, \beta=0.5, d=0.3, e=0.8, \Theta=0.6$.

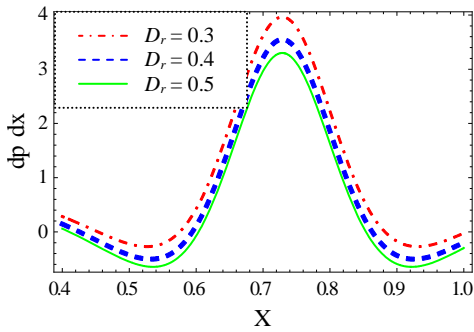


Fig.16. Effect of D_r on the variation of pressure gradient dp/dx with x :
 $b=0.4, a=0.2, \phi=0.2, \mu=1, \eta=1, W_i=0.01, F_r=1, R_e=10, \beta=0.5, d=0.3, e=0.8, \Theta=0.6$.

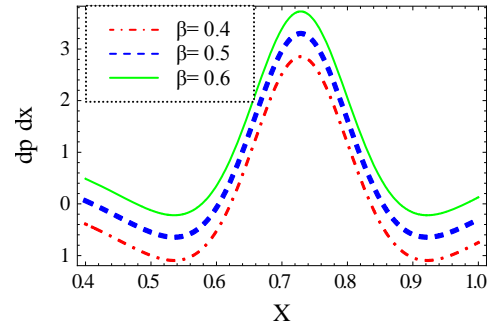


Fig.17. Effect of β on the variation of pressure gradient dp/dx with x :
 $b=0.4, a=0.2, \phi=0.2, \mu=1, \eta=1, W_i=0.01, D_r=0.5, F_r=1, R_e=10, d=0.3, e=0.8, \Theta=0.6$.

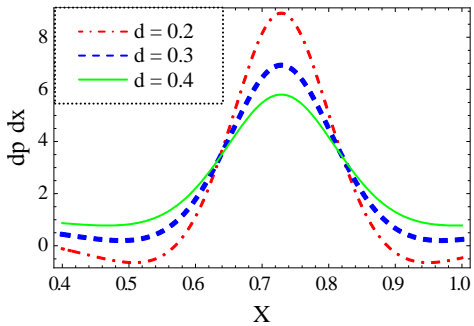


Fig.18. Effect of d on the variation of pressure gradient dp/dx with x :
 $b=0.4, a=0.2, \phi=0.2, \mu=1, \eta=1, W_i=0.01, D_r=0.5, F_r=1, R_e=10, \beta=0.5, e=0.8, \Theta=0.6$.

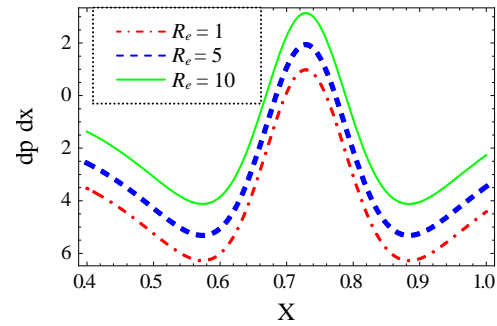


Fig.19. Effect of R_e on the variation of pressure gradient dp/dx with x :
 $b=0.4, a=0.2, \phi=0.2, \mu=1, \eta=1, W_i=0.01, D_r=0.5, F_r=1, \beta=0.5, d=0.3, e=0.8, \Theta=0.6$.

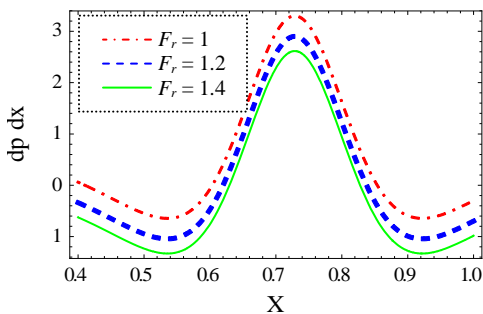


Fig.20. Effect of F_r on the variation of pressure gradient dp/dx with x :
 $b=0.4, a=0.2, \phi=0.2, \mu=1, \eta=1, W_i=0.01, D_r=0.5, R_e=10, \beta=0.5, d=0.3, e=0.8, \Theta=0.6$.

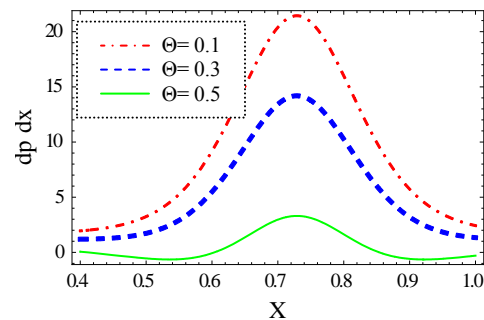


Fig.21. Effect of Θ on the variation of pressure gradient dp/dx with x :
 $b=0.4, a=0.2, \phi=0.2, \mu=1, \eta=1, W_i=0.01, D_r=0.5, F_r=1, R_e=10, \beta=0.5, d=0.3, e=0.8$.

4.3. Trapping phenomenon

Another interesting phenomenon in peristaltic motion is trapping. In the wave frame, streamlines under certain conditions split to trap a bolus which moves as a whole with the speed of the wave. The effect of Weissenberg number W_i on trapping can be seen through Fig.22 for an inclined asymmetric channel. Furthermore, Fig.22 shows that the bolus is anti-symmetric about the center line and its size decreases with an increase in W_i . It is observed from Figs.23 and 24 that the trapped bolus which are moving as whole increases in size with the increase in b and a . The effects of phase shift ϕ on trapping can be seen from Fig.8. It is depicted that increase in ϕ the trapping bolus which is moving as a whole decreases. The effect of Darcy number D_r on the trapping is illustrated in Fig.26 and it is observed that the size of trapped bolus rapidly increases with increasing D_r . Fig.27 depicts the effects of channel width d on trapping. The trapped bolus exists for small values of d , its size decreases with increasing d .

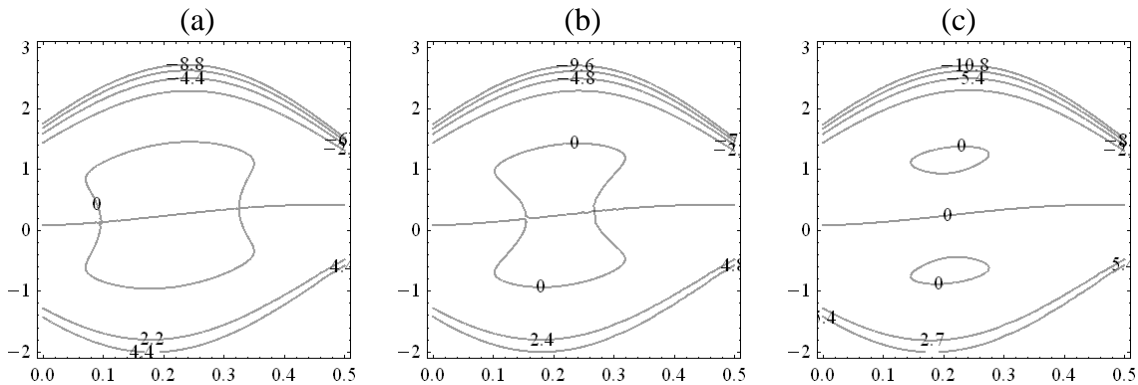


Fig.22. streamlines for $b=0.7, \phi=0.5, a=0.7, \mu=0.01, \eta=0.01, D_r=0.7, \Theta=1.2, d=0.5, e=0.5,$ and for different W_i ; (a) $W_i=1.1,$ (b) $W_i=1.2;$ (c) $W_i=1.3.$

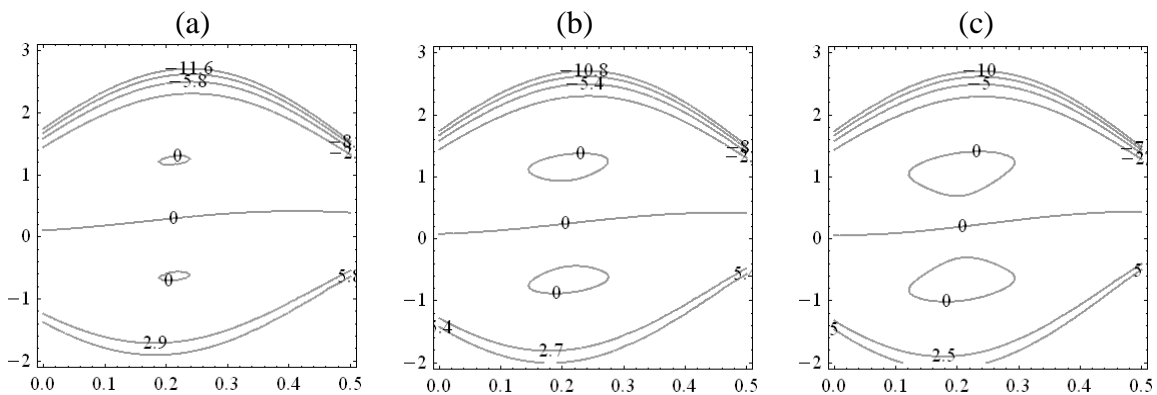


Fig.23. streamlines for $W_i=1.3, \phi=0.5, a=0.7, \mu=0.01, \eta=0.01, D_r=0.7, \Theta=1.2, d=0.5, e=0.5,$ and for different b ; (a) $b=0.6,$ (b) $b=0.7,$ (c) $b=0.8.$

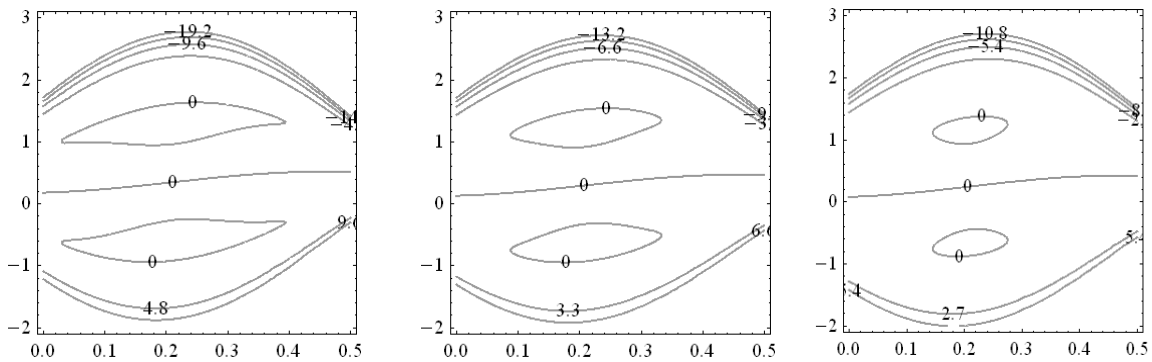


Fig.27. streamlines for $W_i=1.3$, $a=0.7$, $b=0.7$, $\mu=0.01$, $\eta=0.01$, $\phi=0.5$, $\Theta=1.2$, $D_r=0.7$, $e=0.5$, and for different d ; (a) $d=0.3$, (b) $d=0.4$, (c) $d=0.5$.

4.4 Temperature characteristics

The expressions for temperature are given by Eq.(67). To explicitly see the effects of various parameters on temperature, Eq.(67) has been numerically evaluated and the results are presented in Fig.28-34. From Fig.28, it can be found that the temperature profiles are almost parabolic and temperature increases with increase of channel width d . Further, it can be noticed that the increase in Weissenberg number W_i causes a decrease in temperature are plotted in Fig.29. Also Fig.30 display the influence of amplitude ratio of the upper wall on the temperature distribution. We note that temperature increases with increasing a . Fig.31 displays the influence of amplitude ratio of the lower wall on the temperature distribution. It can be noticed that temperature increases when $(1 < \theta < 0.4)$ and decreases when $(1 > \theta > 0.4)$ that occurs by increasing b . The effects increasing Darcy number D_r and Eckert number E_r on the temperature are plotted in Figs.32 and 33, we note that the increasing in D_r and E_r causes increases in temperature. While with the increase in Prandtl number P_r , the temperature field decreases Fig.34.

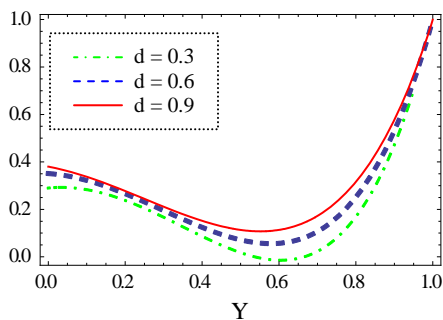


Fig.28. Effect of d on temperature for $b=0.2$, $\phi=\pi/2$, $a=0.2$, $\mu=0.3$, $\eta=0.4$, $W_i=0.7$, $D_r=0.1$, $E_r=-4$, $P_r=1$, $e=0.01$, $x=1$, $\Theta=0.2$.

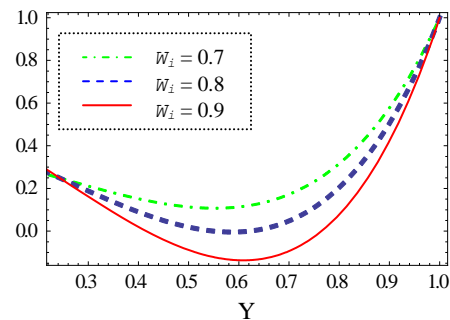


Fig.29. Effect of W_i on temperature for $b=0.2$, $\phi=\pi/2$, $a=0.2$, $\mu=0.3$, $\eta=0.4$, $d=0.3$, $D_r=0.1$, $E_r=-4$, $P_r=1$, $e=0.01$, $x=1$, $\Theta=0.2$.

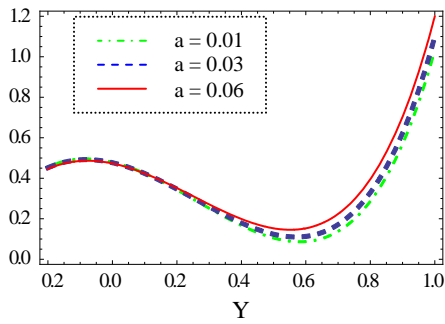


Fig.30. Effect of a on temperature for $b=0.2, \phi= \pi/2, \mu=0.3, \eta=0.4, d=0.3, D_r=0.1, E_r=-4, P_r=1, W_i=0.8, e=0.01, x=1, \Theta=0.2$.

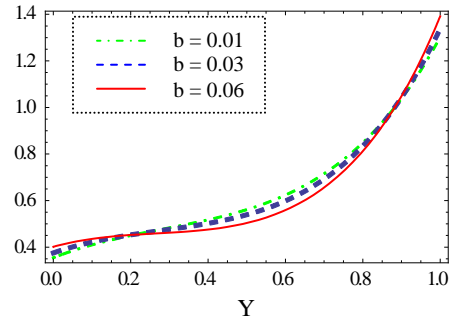


Fig.31. Effect of b on temperature for $a=0.2, \phi= \pi/2, \mu=0.3, \eta=0.4, d=0.3, D_r=0.1, E_r=-4, P_r=1, W_i=0.8, e=0.01, x=0.9, \Theta=0.2$.

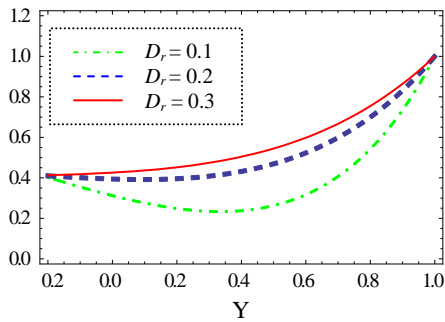


Fig.32. Effect of D_r on temperature for $a=0.2, b=0.2, \phi= \pi/2, \mu=0.3, \eta=0.4, d=1.3, E_r=-4, P_r=1, W_i=0.8, e=0.01, x=0.9, \Theta=0.2$.

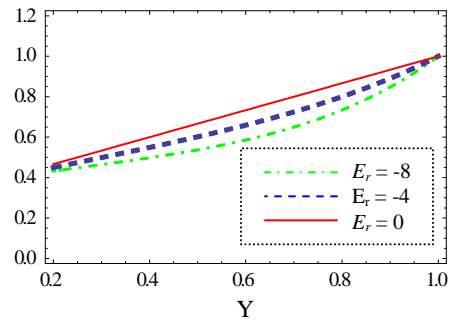


Fig.33. Effect of E_r on temperature for $a=0.2, b=0.2, \phi= \pi/2, \mu=0.3, \eta=0.4, d=0.3, D_r=0.1, P_r=1, W_i=0.8, e=0.01, x=1, \Theta=0.2$.

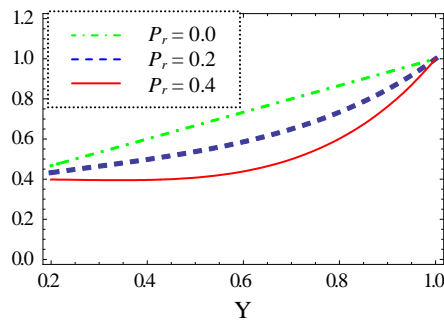


Fig.34. Effect of P_r on temperature for $a=0.2, b=0.2, \phi= \pi/2, \mu=0.3, \eta=0.4, d=0.3, D_r=0.1, x=1, W_i=0.8, e=0.01, E_r=-4, \Theta=0.2$.

5. Concluding remarks

In this paper, we investigated the peristaltic transport of a Johnson-Segalman fluid through a porous medium in an inclined asymmetric 2-D channel under the assumptions of long-wavelength and low-Reynolds number. A perturbation solution for small Weissenberg number is obtained for the stream function, axial pressure gradient, pressure rise and temperature field over a wavelength. It is found that :

- The pressure rise over a wavelength ΔP decreases with an increase in d in the pumping ($\Delta P > 0$) and free pumping ($\Delta P = 0$), while the situation is reversed in the co-pumping region ($\Delta P < 0$).
- The pressure rise over a wavelength ΔP decreases with an increase in Weissenberg number W_i and phase difference ϕ in the pumping region ($\Delta P > 0$), while the situation is reversed in the co-pumping region ($\Delta P < 0$) and free pumping ($\Delta P = 0$).
- The pressure rise over a wavelength ΔP decreases by increasing F_r , while increases by increasing D_r and β .
- The axial pressure gradient decreases by increasing d , F_r , ϕ , η and Θ , while increases by increasing a , b , W_i , R_e , β and μ .
- The size of the trapped bolus increases with an increase in a , b , D_r , while decreases with an increase in W_i , ϕ and d .
- The temperature field increases with the increase in d , a , D_r and E_r , while with the increase in W_i , b and P_r the temperature field decreases.

References

1. Burns . J.C., J. Parkes (1967), Peristaltic motion, J. F. Mech. 29 ,731-743.
2. Brown.T.D.,T.K. Hung (1977), Computational and experimental investigations of two dimensional non-lineare peristaltic flows, J. Fluid Mech. 83, 249-272.
3. Eytan.O.,D.Elad (1999), Analysis of intra-uterine fluid motion induced by uterine contractions, Bull. Math. Biol. 61 221-238.
4. El Shewawey. E. F. and S. Z. A. Hhusseny (2000), Effects of porous boundaries on peristaltic transport through a porous medium, Acta Mechanica, 143, 165-177.
5. El Shehawey E.F., Kh. S. Mekheimer, S. F. Kaldas, and N. A. S. Afifi (1999)., Peristaltic transport through a porous medium, J. Biomath. 14.
6. Fung Y.C., C.S. Yih (1968), Peristaltic transport, J. Appl. mech. 901-905.
7. Hayat. T., Y. Wang, A. M. Siddiqui, K.Hutter (2003), Peristaltic motion of a Johnson-Segalman fluid in a planar channel, Math. Probl. Eng. 1-23.
8. Hayat. T., Y.Wang, K. Hutter, S. Asghar, M. Siddiqui (2004), Peristaltic transport of an oldroyd-B Fluid in a planar channel, Math. Probl. Eng. 4, 347-376.
9. Hayat. T., N. ALI (2006), Peristaltically induced motion of a MHD third grade fluid in Adeformable tube, Physica A 370,225-239.
10. Haroun. M.H (2006), Effect of wall compliance on peristaltic transport of a Newtonian fluid in an asymmetric channel, Mathematical problems in Engineering, doi:10.1155/MPE/61475.
11. Hayat. T., Javed M, Ali N (2008), MHD Peristaltic transport of a Jeffery fluid in a channrl with compliant walls and porous spase. Transp Porous Med 74, 259-274.
12. Hayat. T., Wang Y, Siddiqui AM, Ashgar S (2004), A mathematical model for study of gliding motion of bacte ria on a layer of non-Neotonian slim. Math Method Appl Sci 27, 1447-1468.

13. Hayat. T ., Wang Y, Siddiqui AM, Hutter K, Ashgar (2002), Peristaltic transport of a third order fluid in a circular cylindrical tube. *Math Models Methods Appl Sci* 12, 1691-1706.
14. Hayat. T., Mahomed FM, Ashgar (2005), Peristaltic flow of a magnetohydrodynamic Johnson-Segalman fluid. *Nonlinear Dynamics* 40, 375-385.
15. Haroun. MH (2005), Effect of relaxation and retardation time on peristaltic transport of the Oldroydian viscoelastic fluid. *Journal of Applied Mechanics and Technical Physics* 46 , 842-850.
16. Hayat. T., Ambreen A, Ali. N (2008), Peristaltic transport of a Johnson-Segalman fluid in an asymmetric channel. *Math Comput Model* 47, 380-400.
17. Haroun. M.H., (2007), Non-linear peristaltic flow of a fourth grade fluid in an inclined asymmetric channel. *Comput. Mater. Sci.* 39, 324-333.
18. Hayat. T., N. Ali and S. asghar (2007), Hall effects on aperistaltic motion of a Maxwell fluid in a porous medium, *Physics Letters A*, 363 , 397- 403.
19. Johnson. M. W. Jr. and D. Segalman (1977), A model for viscoelastic fluid behavior which allows nonaffine deformation , *J. non-Newtonian Fluid Mech.* 2, 255–270.
20. Kolkka. R.W., D. S. Malkus, M. G. Hansen (1988), G. R. Ierly, and R. A. Worthing, Spurt phenomenon of the Johnson Segalman fluid and related models, *J. non-Newtonian Fluid Mech.* 29, 303-335.
21. Kraynik. A. M. and W. R. Schowalter (1981), Slip at the wall and extrudate roughness with aqueous solutions of polyvinyl alcohol and sodium borate, *J. Rheol.* 25 , no. 1, 95–114.
22. Lim. F. J. and W. R. Schowalter (1989), Wall slip of narrow molecular weight distribution polybutadienes, *Rheol.* 33 , no. 8, 1359–1382.
23. Latham. T.W (1966), Fluid motion in Peristaltic Pump, M.S. Thesis, MIII, Cambridge, Mass.
24. Malkus. D. S., J. A. Nohel and B. J. Plohr (1990), Dynamics of shear flow of a non-Newtonian fluid, *J. Comput. phys.* 87, no. 2, 464–487.
25. McLeish. T. C. B. and R. C. Ball (1986), A molecular approach to the spurt effect in polymer melt flow, *J. Polym ,Sci. (B)* 24, 1735–1745.
26. Migler. K. B., H. Hervert, and L. Leger (1990), Slip transition of a polymer melt under shear stress, *Phys.. Rev. Leet.* 70 , no. 3, 287–290.
27. Migler. K. B., G. Massey., H. Hervert and L. Leger (1994), The slip transition at the polymer-solid interface, *J. Condens. Matter* 6 , A301–A304.
28. Nadeem, S.; Akbar, N.S, (2010), Influence of heat transfer on peristaltic transport of a Johnson–Segalman fluid in an inclined asymmetric channel. *Commun. Nonlinear Sci. Simulat.* 15, 2860-2877.
29. Naby AEHAE, Misery AEME, Shamy IIE (2003), Hydromagnetic flow of fluid with variable viscosity in unifo rm tube with peristalsis, *J Phys A: Math Gen* 36,, 8535.
30. Naby AEHAE, Misery AEME, Kareem MFAE (2006), Effects of a magnetic field on trapping through peristaltic motion for generalized Newtonian fluid in channel. *Physica A* 367: 79-92.
31. Osnat. E., David. E (1999); Analysis of intra-uterine fluid motion induced by uterine contractions. *Bull Math Biol* 61, 221-238.
32. Pozrikidis. CA. (1987) , A study of peristaltic flow. *J Fluid Mech* 180, 515-527.
33. Ramamurthy. A. V (1986), Wall slip in viscous fluids and influence of materials of construction, *J. Rheol.* 30, no. 2, 337–357.
34. Rao. I. J. and K. R. Rajagopal (1999), Some simple flows of a Johnson-Segalman fluid, *Acta Mech.* 132, no. 1-4, 209–219.
35. Reddy. MS., Raju GSS (2010), Non-linear peristaltic pumping of Johnson- Segalman fluid in an asymmetric channel under the effect of a magnetic field. *European J. os scientific research* 1, 147-164.
36. Srinivas. S.; Pushparaj V. (2008), Non-linear peristaltic transport in an inclined asymmetric channel. *Commun. Nonlinear Sci. Numer. Simul.* 13, 1782–1795.